communications biology
A Nature Portfolio journal

Article

https://doi.org/10.1038/s42003-025-08789-z

Seasonally and niche-differentiated diversity of active, dormant and dead microbes in coastal waters and surface sediments

Yunjun Yu[1], Guanzhe Li[2] ✉, Haoyuan Zhang[2], Zeyu Hu[2], Dirui Yu[2] & Jun Gong[2,3,4] ✉

Metabarcoding surveys have rarely discriminated metabolically active, dormant, and dead microbes in environmental samples. This study employed a triple metabarcoding approach targeting environmental 16S and 18S rRNA genes and their transcripts to investigate the diversity of these physiologically distinct assemblages in the water column and surface sediments of a tropical coastal region. We found that dead bacteria, archaea, and microeukaryotes (relic DNA) accounted for ≤5% of the planktonic DNA pools but significantly contributed to ASV richness (53%, 50%, and 32%, respectively), while dominating in sediments (44% of sequence, 80% of richness). In viable assemblages, dormant microbes were rarer but enriched richness, particularly in the water (20%, 62%, and 28%, respectively). Collectively, the proportions of microbes in different physiological states exhibited niche-specific and seasonal patterns, primarily driven by pH and temperature. Significant differences in richness and assemblage composition were observed between water, sediment, and seasons for all physiological fractions. Active microbial communities responded to distinct environmental drivers compared to DNA-characterized assemblages, suggesting that DNA-based methods may misidentify factors driving functional diversity in biogeochemical cycles. Dormant taxa exhibited a broader taxonomic distribution than previously recognized, underscoring the need for further research on microbial ecophysiology, function, and biogeography across temporal and spatial scales.

In the past two decades, our comprehension of the temporal and spatial dynamics in microbial diversity, community composition, and structure across diverse ecosystems has been significantly advanced through the application of molecular techniques, such as high-throughput sequencing or metabarcoding of 16S, 18S rRNA genes[1–3]. These methodologies predominantly rely on DNA in environmental samples, which is extracted and purified, representing a composite DNA pool from both actively growing and inactive populations, including those from dormant and dead organisms[4,5]. Consequently, metabarcoding of DNA captures a blend of active, deceased, and dormant microbial diversity, potentially leading to an overestimation of the diversity and prevalence of active microbes involved in biogeochemical cycles[6–8]. Although it is increasingly acknowledged that the deceased and dormant microbes (resting spores and cysts) contribute a substantial and variable component to DNA pools in environmental samples[5,6,9–13], and relative quantity of rDNA to rRNA transcripts has been frequently used in assessing microbial activities[14–16], distinguishing active populations from dormant and dead ones (represented by relic DNA), remains a challenge in the application of metabarcoding approaches[13,17–21].

Propidium monoazide (PMA) is a photoreactive dye that only can covalently cross-link to the DNA of dead (broken) cells upon light exposure, rendering the DNA insoluble and precipitated with cell debris during DNA extraction, so that only the DNA from viable cells is retained and successfully amplified during PCR[6,22–25]. To further discriminate active and dormant microbes in the viable community, recently we have developed the

---

[1]South China Institute of Environmental Sciences, Ministry of Ecology and Environment, Guangzhou, China. [2]School of Marine Sciences, Sun Yat-sen University, Zhuhai, China. [3]Southern Marine Science and Engineering Guangdong Laboratory (Zhuhai), Zhuhai, China. [4]Guangdong Provincial Key Laboratory of Marine Resources and Coastal Engineering, School of Marine Sciences, Sun Yat-sen University, Zhuhai, China. ✉e-mail: ligzh29@mail2.sysu.edu.cn; gongj27@mail.sysu.edu.cn

triple metabarcoding approach (TMA), which integrates the metabarcoding of the total environmental rDNA pool (DNA-seq), the rRNA pool (RNA-seq), and DNA treated with propidium monoazide (PMA-seq) to categorize the phylotypes detected within a given DNA pool into dead, dormant, and active fractions[26]. The theoretical assumptions of TMA are as follows: (1) The phylotypes detected in DNA-seq are derived from all active, dormant, and dead cells. (2) PMA-seq targets populations with intact cell membranes, namely dormant and active ones. (3) The ratio of rRNA to rDNA varies with cell size, which also differs greatly from species to species and may inversely relates to cell activity[27,28]. The use of the ratio of relative abundances of rRNA to relative abundance of rDNA (i.e., rRNA%: rDNA%) could lead to a high mis-classification error of assigning active populations to dormant[29]. Therefore, we apply an absolute definition of dormancy. Due to low cellular activity, rRNA transcripts in dormant cells are too rare to be detectable in RNA-seq. Thus, phylotypes present in both DNA-seq and PMA-seq but absent in RNA-seq are considered dormant. Our definition may exclude some viable phylotypes with slow growth rates or low metabolical activity (i.e., those with few rRNA transcripts), but it is conservative to minimize the risk of misclassifying populations in transitional physiological states as dormant. (4) Phylotypes detected in both DNA-seq and RNA-seq are considered to be from active cells. (5) Phylotypes present in DNA-seq but absent in both PMA-seq and RNA-seq are derived from dead cells. The application of TMA has revealed previously unobserved insights into the diversity, relative quantity in DNA pools, assemblage structure, and environmental drivers of the physiologically distinct fractions of benthic microeukaryotes[26]. However, the physiology-based perspective of bacterial and archaeal diversity has yet to be elucidated using TMA, despite the rationale behind TMA being applicable to all prokaryotic and eukaryotic microorganisms.

Essential inquiries regarding microbial diversity across diverse systems still need to be explored within the framework of differentiating active, dormant, and dead populations. In planktonic microbial diversity studies, water samples are typically filtered to collect microbial biomass, potentially excluding dissolved extracellular DNA but retaining that adsorbed onto particles and debris from dead cells, which are then sequenced[30]. Furthermore, variations in water's physiochemical properties, such as salinity, temperature, pH, light, and nutrient availability, due to depth gradients, seasonal changes, and the mixing of saline and freshwater, may also selectively induce dormancy, resuscitation, and even death among microbial populations[11,31].

In this study, employing TMA, we investigated the diversity and ecophysiology of bacteria, archaea, and microeukaryotes in the surface and bottom waters and surface sediments of a shallow coastal region influenced by freshwater. We focused on niche-wise differentiation and seasonality, hypothesizing that: (1) there is a significant seasonality in diversity and quantity of dead and dormant microbes in the water column, even when DNA pools were obtained through filtering; (2) planktonic microbial systems differ from benthic systems in many aspects and there are marked differences between surface and bottom water layers due to depth gradients of many physicochemical variables; and (3) traditional total DNA-based microbial diversity and assemblage structure exhibited spatial and seasonal patterns that differed from those of active microbes (Supplementary Fig. 1).

Results

Amplicon sequence variant (ASV) richness of active, dormant, and dead microbes in the rDNA pools

In general, a subset of viable ASVs was consistently identified as dormant within the water columns across both seasons, representing approximately 20%, 62%, and 28% of the viable bacterial, archaeal, and microeukaryotic ASVs, respectively (Fig. 1A). These percentages were considerably lower in sediments, at 11%, 14% and 9% (Fig. 1B). In contrast, consistently active ASVs constituted higher proportions in sediments (71%, 71%, and 81%) compared to water columns (45%, 5%, and 28%) (Fig. 1A, B).

Across the total rDNA pools of water and sediment samples in both summer and winter, dormant and dead microbial ASVs (>50%) were more prevalent than active ones (<50%) (Fig. 1C–E and Supplementary Fig. 2; Table 1). The proportion of ASV numbers of these different fractions in rDNA pools varied significantly, exhibiting distinct niche-dependent patterns (Fig. 1C–E and Supplementary Table 1). Active bacteria, archaea, and microeukaryotes were consistently more abundant in water than in sediment rDNA pools (Mann–Whitney *U* test, $p < 0.05$ in all cases; Fig. 1C–E). Similar trends were observed for the dormant fractions in pelagic versus the benthic environments. Conversely, the dead fractions of bacteria, archaea, and microeukaryotes comprised over three-quarters of the richness in the sediments, significantly higher than those in the pelagic environment (Mann–Whitney *U* test, $p < 0.05$ in all cases; Fig. 1C–E).

Niche-wise differences in richness proportions in the rDNA pools were generally small between surface and bottom water layers, but still statistically significant for several fractions (Mann–Whitney *U* test, $p < 0.05$; Fig. 1C–E). Seasonal differences in richness proportions in the rDNA pools were common and niche-dependent. In surface waters, active bacteria, archaea, and microeukaryotes had consistently higher proportions in winter than in summer (Mann–Whitney *U* test, $p < 0.05$; Fig. 1C–E). Similar seasonal patterns were observed for active bacteria and microeukaryotes in the benthos (Mann–Whitney *U* test, $p < 0.05$; Fig. 1C, E). Nevertheless, in bottom waters, lower proportions in winter were detected for active bacteria and active microeukaryotes (Mann–Whitney *U* test, $p < 0.05$, Fig. 1C–E), except for active archaea (Mann–Whitney *U* test, $p < 0.05$; Fig. 1D). The richness proportions of dead fractions showed generally the opposite trend to the active ones, regardless of the three niches (Fig. 1C–E). Seasonal shifts in richness proportions of the dormant fractions in the rDNA pools were generally not significant in surface waters and sediments (Fig. 1C–E). The only exception was in bottom waters, where dormant microeukaryotes accounted for 16% in winter (vs. 8% in summer, Mann–Whitney *U* test, $p < 0.05$; Fig. 1E).

Relative abundances of active, dormant, and dead fractions in the rDNA pools

Despite their relatively low ASV richness, active bacteria and archaea, and microeukaryotes exhibited high relative abundances, constituting 50% to 92% of the rDNA pools, with a notably higher percentage in the waters (on average 85%) compared to sediments (52%) (Fig. 1F–H; Supplementary Fig. 3; Table 1; and Supplementary Table 1). In contrast, the dead fractions were less abundant in the waters (4.6%) than in the benthos (44%) across both seasons (Mann–Whitney *U* test, $p < 0.05$; Fig. 1F–H). No significant differences in relative abundance were observed between the two water layers for these active microbial fractions (Mann–Whitney *U* test, $p > 0.05$; Fig. 1F–H). The dormant archaea (20% vs. 4.0%) and microeukaryotes (7.4% vs. 4.8%) had significantly higher relative abundances in the plankton than in the sediment rDNA pools (Mann–Whitney *U* test, $p < 0.05$; Fig. 1G, H). Additionally, dormant archaea were more abundant in bottom waters than in surface waters (26% vs. 15%, Mann–Whitney *U* test, $p < 0.05$; Fig. 1G).

A significant summer-winter shift in relative abundance was observed for both active (90% vs. 94%) and dormant bacteria (4.7% vs. 1.8%) in surface water rDNA pools. Similar seasonal patterns were also evident in benthic rDNA pools, with lower proportions of active bacteria (40% vs. 62%) and microeukaryotes (44% vs. 61%), and higher proportions of dormant bacteria (6.6% vs. 3.0%), and dead bacteria (53% vs 35%) and microeukaryotes (47% vs. 39%) in summer (Mann–Whitney *U* test, $p < 0.05$; Fig. 1F, H). Conversely, in bottom water rDNA pools, active bacteria (94% vs. 90%) and microeukaryotes (94% vs. 85%), and dormant archaea (34% vs. 18%) had higher relative abundance in summer (Mann–Whitney *U* test, $p < 0.05$; Fig. 1F–H). However, both water layers had similar proportions of dead microbes in their rDNA pools (Mann–Whitney *U* test, $p > 0.05$; Fig. 1F–H), and seasonal variations in the sequence proportion of dormant microeukaryotes were not significant in any of these niches (Fig. 1H).

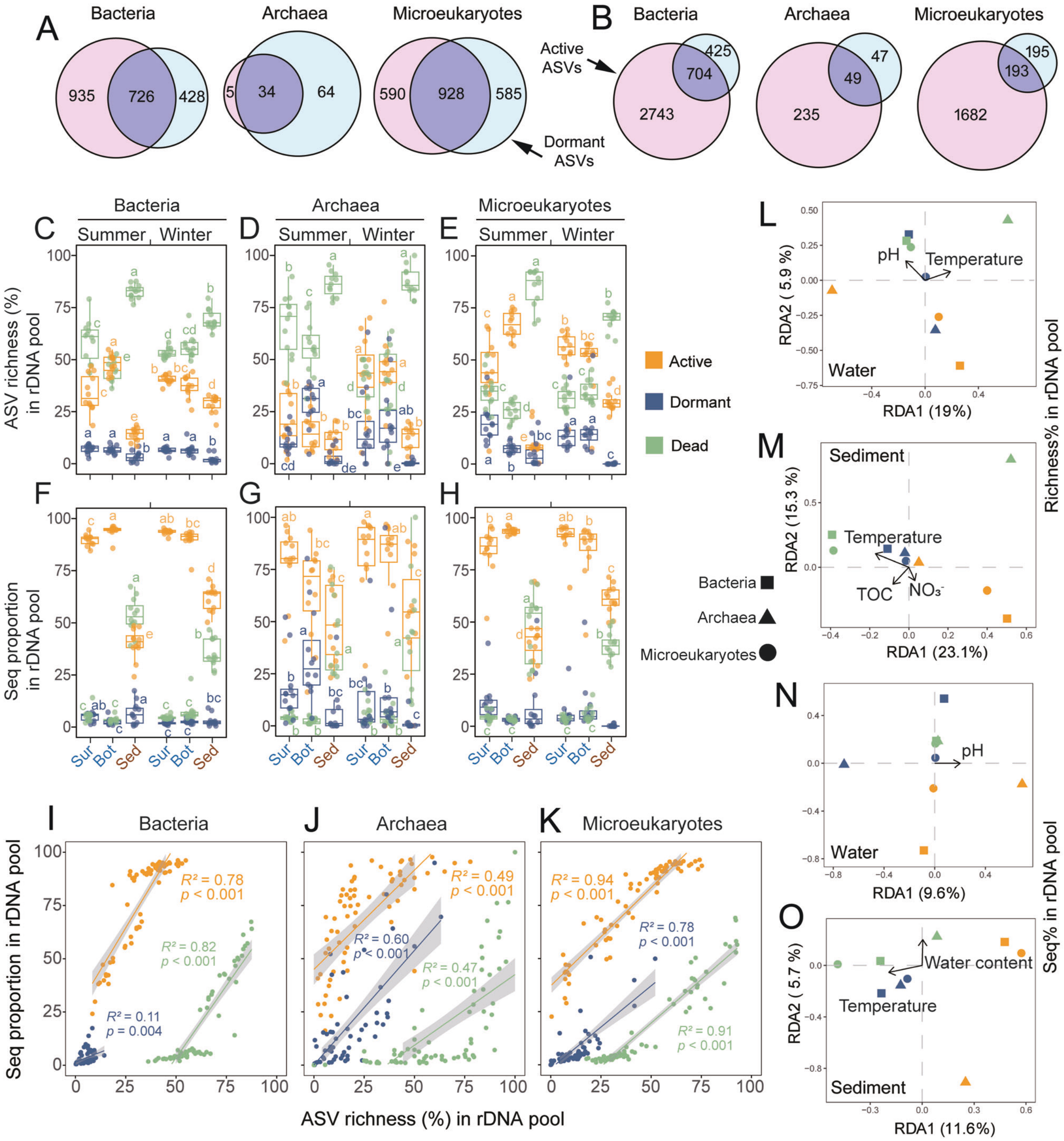

Fig. 1 | Distribution of active, dormant, and dead microbial ASVs in water- and sediment-derived rDNA pools and their environmental drivers. Venn diagrams displaying the counts of ASVs assigned to active and dormant states for bacteria, archaea, and microeukaryotes in (**A**) waters and (**B**) sediments; overlapping sections denote ASVs assigned to active and dormant states at least once. Box plots of ASV richness proportions (**C**–**E**) and sequence abundance proportions (**F**–**H**) for active, dormant, and dead fractions across surface waters (Sur), bottom waters (Bot), and surface sediments (Sed) in two seasons, $n = 12$ biologically independent samples; non-overlapping lowercase letters indicate significant differences between niches or seasons ($p < 0.05$). **I**–**K** Scatter plots revealing positive correlations between sequence number proportions and ASV richness proportions of each physiological fraction, $n = 72$ biologically independent samples. **L**–**O** Redundancy analysis (RDA) ordinations identifying environmental factors significantly associated with shifts in ASV richness proportions (**L** and **M**) and sequence abundance proportions (**N** and **O**) of the three fractions in environmental rDNA pools.

Environmental drivers of the fraction proportions in the rDNA pools

The richness proportion was significantly and positively correlated with the sequence proportion of a given fraction in bacterial, archaeal and microeukaryotic rDNA pools ($R^2 = 0.11$–0.94; $p < 0.005$; Fig. 1I–K), suggesting that variations in both proportions might be driven by similar environmental factors. Indeed, this hypothesis was supported by the RDA plots, which showed that pH and/or temperature were the most significant among several environmental factors that co-varied with richness and sequence proportions of the active, dormant, and dead fractions in the total plankton and benthic rDNA pools ($p < 0.05$; Fig. 1L–O). The importance of pH and temperature was also recognized in correlations between individual fractions and environmental factors (Supplementary Fig. 4). In addition, other factors, including DSi, NO_2^-, SRP: DSi, and SRP, were significant in

Table 1 | Comparisons of ASV richness and read proportions of each fraction in the microbial rDNA pools across summer and winter

	Surface water ($n = 24$)	Bottom water ($n = 24$)	Sediment ($n = 24$)	p
Bacteria, richness%				
Active	37.1 ± 7.1^{b}	42.6 ± 7.3^{a}	21.3 ± 8.3^{c}	<0.001
Dormant	6.8 ± 1.8^{a}	6.6 ± 2.3^{a}	2.8 ± 2.3^{b}	<0.001
Dead	56.1 ± 7.8^{b}	50.8 ± 7.7^{c}	75.9 ± 8.0^{a}	<0.001
Bacteria, reads proportion%				
Active	91.7 ± 2.8^{a}	92.1 ± 4.4^{a}	50.8 ± 12.8^{b}	<0.001
Dormant	$3.2 \pm 2.1^{a,b}$	2.5 ± 1.3^{b}	4.8 ± 4.5^{a}	0.028
Dead	5.1 ± 2.3^{b}	5.4 ± 4.2^{b}	44.4 ± 11.9^{a}	<0.001
Archaea, richness%				
Active	32.2 ± 19.1^{a}	29.0 ± 20.1^{a}	11.6 ± 6.3^{b}	<0.001
Dormant	14.4 ± 13.6^{b}	25.0 ± 14.4^{a}	1.6 ± 3.0^{c}	<0.001
Dead	53.4 ± 18.3^{b}	46.0 ± 19.3^{b}	86.8 ± 6.4^{a}	<0.001
Archaea, reads proportion%				
Active	80.4 ± 17.5^{a}	70.2 ± 25.8^{a}	51.8 ± 22.7^{b}	<0.001
Dormant	14.7 ± 17.5^{b}	25.9 ± 26.1^{a}	4.0 ± 9.4^{b}	<0.001
Dead	4.9 ± 3.7^{b}	3.9 ± 5.3^{b}	44.2 ± 23.1^{a}	<0.001
Microeukaryotes, richness%				
Active	49.3 ± 15.0^{b}	57.9 ± 14.1^{a}	20.1 ± 11.9^{c}	<0.001
Dormant	17.3 ± 9.1^{a}	11.9 ± 9.5^{b}	2.7 ± 5.2^{c}	<0.001
Dead	33.4 ± 7.2^{b}	30.2 ± 6.8^{b}	77.2 ± 10.6^{a}	<0.001
Microeukaryotes, reads proportion%				
Active	87.5 ± 10.2^{a}	89.2 ± 10.8^{a}	52.3 ± 13.9^{b}	<0.001
Dormant	8.5 ± 8.8	6.3 ± 9.8	4.8 ± 11.4	0.450
Dead	4.0 ± 1.8^{b}	4.5 ± 2.9^{b}	42.9 ± 13.0^{a}	<0.001

The p values were obtained using ANOVA; and the superscripts (a, b and c) sharing no letters indicate significant differences using multiple comparisons ($p \le 0.05$).

explaining the variations in richness or sequence proportions of the fractions in rDNA pools (Supplementary Fig. 5).

Spatial and seasonal variations in ASV richness of active, dormant, and dead assemblages

Upon categorizing active, dormant, and dead ASVs across all the samples, we examined the ASV richness and assemblage composition of these activity-different microbes, revealing distinct patterns among niches and between two seasons (Fig. 2A–C, I–K, Q–S and Supplementary Data 1 and 2). Our comparisons indicated that many of the variation patterns in ASV richness and other alpha diversity estimators identified based on active assemblages did not align with those derived solely from the DNA-seq datasets (Fig. 2D, L, T and Supplementary Fig. 6). For instance, active bacterioplankton and microeukaryotes in summer bottom waters were significantly richer than those in summer surface waters (48.0 ± 4.6% vs. 33.9 ± 8.9%; and 66.8 ± 6.4% vs. 44.7 ± 16.0%; Mann–Whitney U test, $p < 0.05$; Fig. 2A, Q), a difference that was not apparent when based on DNA-seq alone (Fig. 2D, T). Furthermore, significant seasonal differences in ASV richness were observed for active bacterioplankton in surface waters (Mann–Whitney U test, $p < 0.05$; Fig. 2A) and for active archaea in sediments (Mann–Whitney U test, $p < 0.05$; Fig. 2I), differences that were not significant using the traditional DNA-based approach (Mann–Whitney U test, $p > 0.05$; Fig. 2L). In addition, based on total rDNA data, bottom water microeukaryotes appeared to be richer in winter than in summer (Mann–Whitney U test, $p < 0.05$; Fig. 2T), a difference that was not significant for the active microeukaryotes identified using the triple metabarcoding approach (Mann–Whitney U test, $p > 0.05$; Fig. 2Q).

Overall, the majority of bacterial, archaeal, and microeukaryotic taxa (phyla and ASV) exhibited physiological shifts between active and dormant states, providing evidence that dormant microbes are phylogenetically widespread. Dormancy was identified at least once for most of the 53 active bacterial phyla except for FCPU426, LCP-89, *Poribacteria*, *Methylomirabilota*, GN01, WS2, and *Abditibacteriota*, for 8 out of the 10 active archaeal phyla (except for *Aenigmarchaeota* and *Altiarchaeota*), and for 24 out of 28 microeukaryotic phyla (except for *Metamonada*, *Rhodelphidia*, *Discosea*, and *Perkinsea*) (Fig. 2). Dormant bacteria exhibited similar richness across water and sediment and between seasons (Fig. 2B). For both dormant archaea and microeukaryotes, however, surface-bottom differences in richness were found, but only in summer (Fig. 2J, R); and seasonal differences in richness were detected only in bottom waters (Fig. 2J, R).

The benthos consistently harbored a more diverse array of dead microbes than the plankton (Fig. 2C, K, S). Surface-bottom and seasonal differences in dead ASV richness were generally insignificant (Fig. 2K, S), except for bacteria, which were more diverse in surface water than in bottom water in summer, and in winter than in summer in the bottom waters (Fig. 2C). Similarly, communities based on total DNA appeared to differ from active ones in terms of the relative abundance of many major taxa (Fig. 2H, P, X).

Assemblage structures of active, dormant, and dead microbes

The assemblage structures of the active, dormant, or dead microbes showed significant differences between water and sediment in either or both seasons, and exhibited distinct seasonality in both waters and sediments (ANOSIM, $p \le 0.05$; Fig. 3 and Table 2). However, the differences in assemblage structure of planktonic microbes of either physiological state in the shallow coastal area were often not significant between surface and bottom water layers (ANOSIM, $p > 0.05$; Fig. 3; Supplementary Fig. 7; and Table 2), except for the dormant and/or dead ones in summer (ANOSIM, $p \le 0.05$; Table 2). Active and dormant archaea in the sediments displayed similar assemblage structure between summer and winter (ANOSIM, $R < 0.07$, $p > 0.05$; Table 2). Although the niche-wise and seasonal variational patterns of the assemblage structures of bacteria, archaea, and microeukaryotes based solely on DNA-seq data were also significant (Supplementary Fig. 7), their R static values were either higher or lower than those of the active fractions (Table 2). There were significant differences in assemblage structure between the DNA-based and the active ones (Supplementary Table 2), indicating that the mixing DNA-based data of dormant and dead microbes with active ones affected the accuracy of characterizing spatial and seasonal changes in assemblage structure of active microbes.

Some major taxa exhibited significantly different relative abundances among active and dormant, and dead assemblages across both seasons (Fig. 2E–G, M–O, U–W). More specifically, planktonic *Alphaproteobacteria*, *Cyanobacteria*, and *Bacteroidota*, Marine Group II, *Mediophyceae*, *Ciliophora*, *Cryptophyceae*, *Mamiellophyceae* were more abundant in active assemblages, whereas *Actinobacteria*, *Planctomycetota*, *Verrucomicrobiota*, *Ca. Nitrosopumilus*, *Dinoflagellata*, *Cercozoa*, and *Fungi* were less represented relative to their dormant counterparts (in all cases, Mann–Whitney U test, $p \le 0.05$; Fig. 4A–C and Supplementary Table 3). In the benthos, *Gammaproteobacteria*, *Nitrospirota*, *Gemmatimonadota*, *Halobacterota*, *Mediophyceae*, *Bacillariophyceae*, *Ciliophora* were more abundant in active than in dormant assemblages, whereas *Acidobacteriota*, *Chloroflexi*, *Firmicutes*, *Nanoarchaeota*, Marine Group III, Marine Benthic Group D, and DHVEG.1, *Dinoflagellata*, *Cercozoa*, and *Cryptophyceae*, *Fungi* were less abundant (most, Mann–Whitney U test, $p \le 0.05$; Fig. 4D–F and Supplementary Table 3).

In both active and dormant assemblages, many microbial taxa showed distinct sequence proportions between plankton and benthos across two seasons, indicating habitat-dependent community assembly of both active and dormant microbes (Fig. 4G–L and Supplementary Data 3). Active *Alphaproteobacteria*, *Cyanobacteria*, *Bacteroidota*, Marine Group II, *Cryptophyceae*, *Mamiellophyceae*, and *Prymnesiophyceae* had higher sequence proportions in planktonic assemblages relative to the benthic counterparts

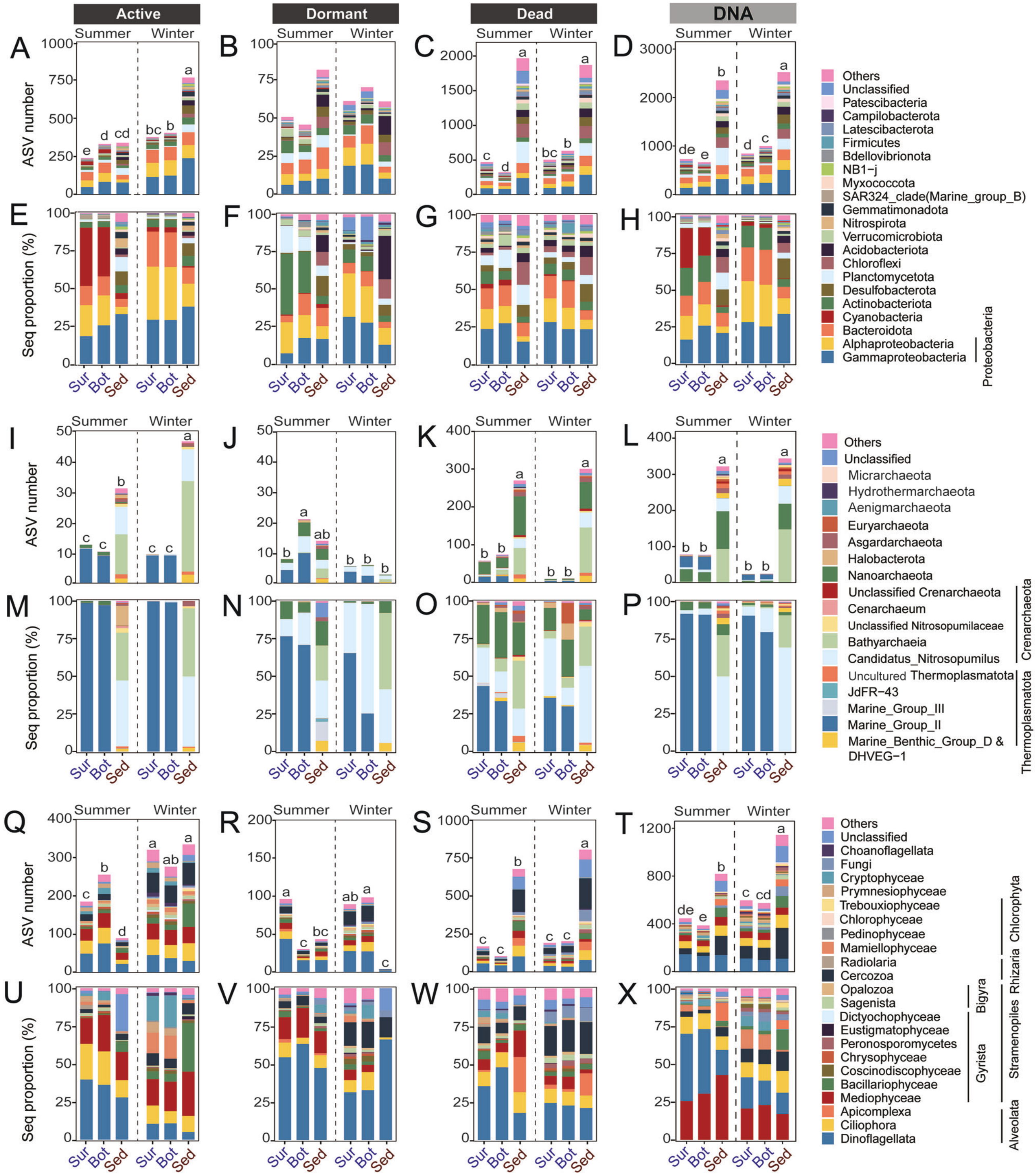

Fig. 2 | Habitat- and season-dependent diversity and compositional shifts in physiologically resolved versus bulk rDNA-defined microbial communities across surface waters (Sur), bottom waters (Bot) and surface sediments (Sed). **A–H** Bacteria. **I–P** Archaea. **Q–X** Microeukaryotes. The ASV numbers were calculated based on rarefied data; distinct lowercase letters denote significant differences between niches or seasons ($p < 0.05$), $n = 12$ biologically independent samples.

(Mann–Whitney *U* test, $p \leq 0.05$; Fig. 4G–I), whereas other active members, such as *Gammaproteobacteria*, *Actinobacteria*, *Planktomycetota*, *Desulfobacterota*, *Nitrospirota*, *Acidobacteriota*, *Gemmatimonadota*, Ca. *Nitrosopumilus*, *Bathyarchaeia*, and *Halobacterota* exhibited lower sequence proportions (Mann–Whitney *U* test, $p \leq 0.05$; Fig. 4G–I). In dormant assemblages, *Alphaproteobacteria*, *Actinobacteria*, *Verrucomicrobiota*, Marine Group II, *Ciliophora*, and *Bacillariophyceae* had higher sequence proportions in plankton than in benthos (Mann–Whitney *U* test, $p \leq 0.05$; Fig. 4J–L), whereas *Acidobacteriota*, *Chloroflexi*, *Desulfobacterota*, *Firmicutes*, *Nitrospirota*, *Bathyarchaeia*, Marine Benthic Group D, and DHVEG.1, *Asgardarchaeota*, *Cercozoa*, and *Fungi* were less abundant (Mann–Whitney *U* test, $p \leq 0.05$; Fig. 4J–L and Supplementary Data 3).

Seasonally, many taxa had significantly different sequence proportions in both the active and dormant assemblages (Fig. 5). The number of taxa exhibiting significant seasonal shifts in the dormant assemblages was comparable to those in the active ones in water columns (Fig. 5A–F),

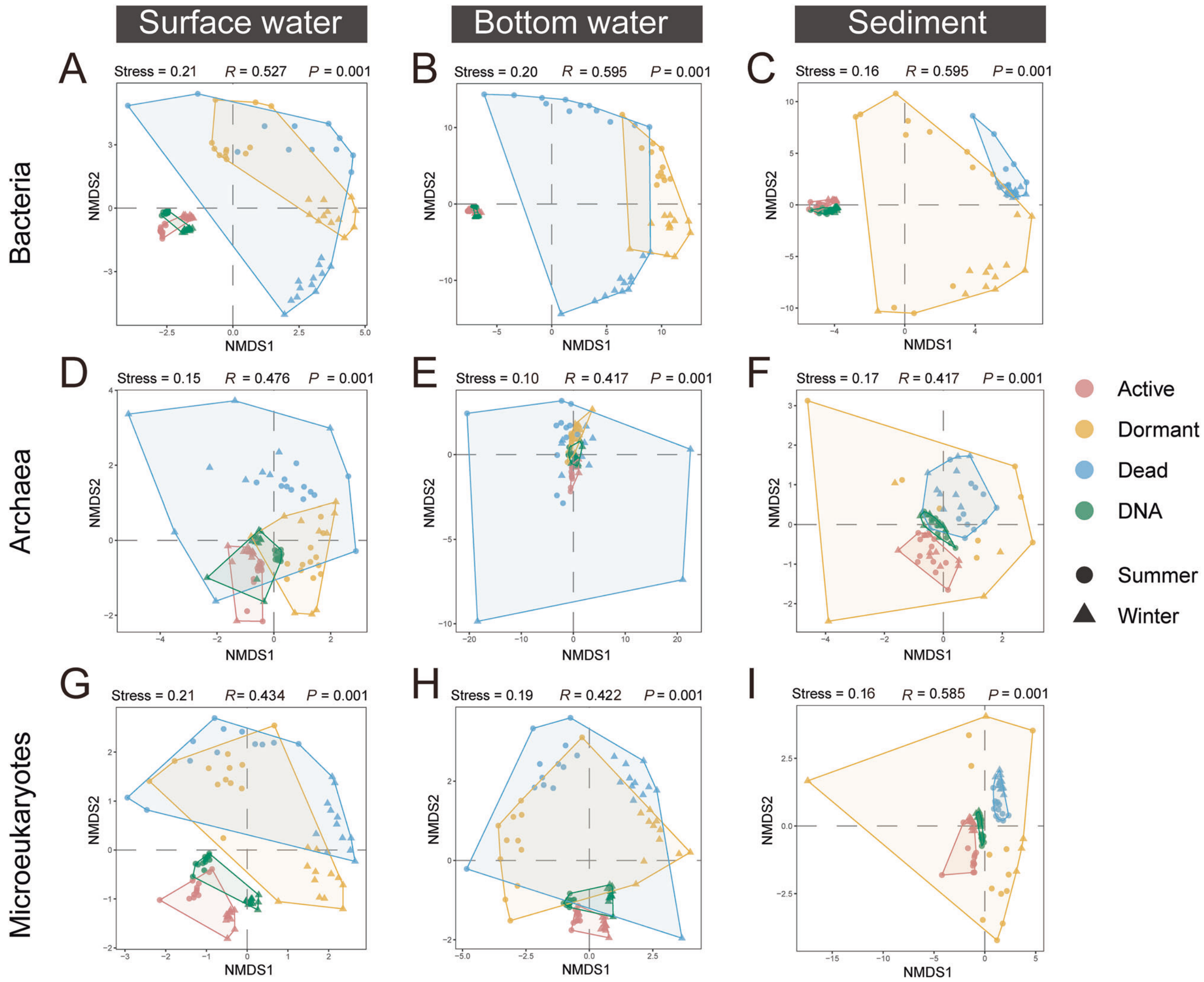

Fig. 3 | Niche- and season-dependent variations in assemblage structure of physiologically distinct microbial fractions. Non-metric multidimensional scaling (NMDS) ordinations illustrate compositional variations in bacterial (**A**–**C**), archaeal (**D**–**F**), and microeukaryotic (**G**–**I**) assemblages resolved into active, dormant, dead, and bulk environmental rDNA pools. All ordinations achieve acceptable representations (stress ≤ 0.21). ANOSIM global *R* and *p*-values are provided to quantify the significance of observed differences.

whereas the former was much lower than the latter in the benthos (Fig. 5G–L), indicating more pronounced seasonality of dormant assemblages in waters than in sediments. Planktonic *Cyanobacteria*, SAR324/Marine Group B, *Bdellovibrionota*, *Myxococcota*, and *Dinoflagellata* in the active and dormant assemblages consistently had higher relative abundance in summer than in winter, whereas *Gammaproteobacteria*, *Alphaproteobacteria*, *Desulfobacterota*, *Camplilobacterota*, *Cercozoa*, *Coscinodiscophyceae*, *Opalozoa*, *Peronosporomycetes*, *Choanoflagellata*, and *Fungi* consistently showed the opposite (Mann–Whitney *U* test, $p \leq 0.05$; Fig. 5A–F and Supplementary Data 3). Furthermore, planktonic *Actinobacteria*, *Planctomycetota*, *Verrucomicrobiota*, Marine Group II, and *Apicomplexa* in the dormant assemblages were more abundant in summer than in winter, while *Gemmatimonadota*, *Firmicutes*, *Acidobacteriota*, Ca. *Nitrosopumilus*, *Halobacterota*, *Sagenista*, and *Chrysophyceae* displayed the opposite (Mann–Whitney *U* test, $p \leq 0.05$; Fig. 5D–F and Supplementary Data 3).

The relative abundances of major lineages within the phyla *Acidobacteriota* and *Nanoarchaeota* in active and dormant assemblages exhibited distinct seasonal patterns and varied between the two niches (Fig. 6). Both active and dormant acidobacteria were predominantly represented by Subgroups 10 and 23 (Class *Thermoanaerobaculia*) and Subgroup 17 (Class *Vicinamibacteria*). Acidobacterial Subgroup 22 was relatively abundant in sediments but not in water columns. Other dormant and abundant acidobacteria in sediments included Subgroup 9, *Aminicenantales* (Class *Aminicenantia*), Subgroup 7 (Class *Holophagae*), and Subgroup 21. Seasonally, many of these acidobacteria, in both active and dormant assemblages, were frequently more abundant in winter than in summer (Fig. 6A).

Nanoarchaeota was dominated by genus *Woesearchaeales* in both water and sediments (Fig. 6B). In water columns, this genus exhibited significant seasonality, with higher abundance in summer than in winter in both active and dormant assemblages (Mann–Whitney *U* test, $p < 0.05$). In certain summertime sediment samples, *Woesearchaeales* was also abundant, but seasonal differences were not statistically significant (Mann–Whitney *U* test, $p > 0.05$; Fig. 6B).

Environmental drivers of diversity and assemblage structures of the active, dormant, and dead microbes

The ASV richness of active bacteria, archaea and microeukaryotes in both water and sediment were correlated significantly with distinct sets of environmental factors, which often differed from those associated with total DNA-based ASV richness (Fig. 7). Water depth was significantly and positively correlated with the richness of active bacterioplankton ($\rho = 0.416$, $p = 0.003$), but not with that of the total DNA-based richness of bacterioplankton (Fig. 7A). Temperature was negatively correlated with the

Table 2 | Comparisons of assemblage structure of active, dormant, and dead microbes between niches and seasons

		Niche			Seasonality (Summer vs. Winter)		
		Both seasons (*n* = 24)	**Summer only (*n* = 12)**	**Winter only (*n* = 12)**	**Surface water (*n* = 12)**	**Bottom water (*n* = 12)**	**Sediment (*n* = 12)**
Bacteria							
Active	S_water vs. B_water	−0.01	0.06	0.02	**1.00****	**1.00****	**0.64**
	S_water vs. Sediment	**0.74****	**0.99****	**0.99****			
	B_water vs. Sediment	**0.74****	**0.99****	**0.99****			
Dormant	S_water vs. B_water	0.02	**0.22****	−0.03	**0.77****	**0.71****	**0.41**
	S_water vs. Sediment	**0.52****	**0.66****	**0.91****			
	B_water vs. Sediment	**0.58****	**0.70****	**0.92****			
Dead	S_water vs. B_water	**0.06**	**0.22***	**0.13***	**0.68****	**0.83****	**0.35**
	S_water vs. Sediment	**0.44****	**0.70****	**0.74****			
	B_water vs. Sediment	**0.45****	**0.89****	**0.63****			
DNA	S_water vs. B_water	0.00	**0.16***	−0.01	**0.99****	**1.00****	**0.40**
	S_water vs. Sediment	**0.93****	**1.00****	**0.99****			
	B_water vs. Sediment	**0.92****	**1.00****	**0.99****			
Archaea							
Active	S_water vs. B_water	−0.01	0.07	−0.03	**0.46****	**0.57****	0.05
	S_water vs. Sediment	**0.98****	**0.99****	**0.99****			
	B_water vs. Sediment	**0.97****	**0.99****	**0.99****			
Dormant	S_water vs. B_water	0.01	0.02	0.01	**0.56****	**0.46****	0.06
	S_water vs. Sediment	**0.71****	**0.76****	**0.07***			
	B_water vs. Sediment	**0.69****	**0.73****	**0.69***			
Dead	S_water vs. B_water	**0.06***	**0.16****	0.03	**0.34****	**0.13***	**0.16***
	S_water vs. Sediment	**0.40****	**0.77****	**0.34****			
	B_water vs. Sediment	**0.31****	**0.36****	**0.34****			
DNA	S_water vs. B_water	−0.03	−0.07	−0.02	**0.67****	**0.73****	**0.08****
	S_water vs. Sediment	**0.95****	**1.00****	**0.92****			
	B_water vs. Sediment	**0.93****	**1.00****	**0.88****			
Microeukaryotes							
Active	S_water vs. B_water	−0.01	0.09	−0.01	**1.00****	**1.00****	**0.67****
	S_water vs. Sediment	**0.21***	**0.69***	**0.96****			
	B_water vs. Sediment	**0.20****	**0.35****	**0.95****			
Dormant	S_water vs. B_water	0.01	**0.18***	−0.04	**0.86****	**0.88****	**0.28**
	S_water vs. Sediment	**0.31****	**0.14***	**0.89***			
	B_water vs. Sediment	**0.23****	**0.33****	**0.38**			
Dead	S_water vs. B_water	−0.02	**0.10**	0.02	**0.84****	**0.80****	**0.84****
	S_water vs. Sediment	**0.44****	**0.62****	**0.82****			
	B_water vs. Sediment	**0.45****	**0.84****	**0.63****			

Table 2 (continued) | Comparisons of assemblage structure of active, dormant, and dead microbes between niches and seasons

		Niche			Seasonality (Summer vs. Winter)		
		Both seasons ($n = 24$)	Summer only ($n = 12$)	Winter only ($n = 12$)	Surface water ($n = 12$)	Bottom water ($n = 12$)	Sediment ($n = 12$)
DNA	S_water vs. B_water	−0.02	0.07	−0.05	**1.00****	**1.00****	**0.86****
	S_water vs. Sediment	**0.44****	**0.84****	**0.99****			
	B_water vs. Sediment	**0.52****	**0.91****	**0.99****			

The values are R static obtained using ANOSIM. Bold values indicate statistically significant differences ($p \le 0.05$), and * and ** indicate $p \le 0.01$ and ≤ 0.001, respectively. S_water, surface water; B_water, bottom water.

richness of active benthic bacteria ($\rho = -0.734$, $p < 0.001$), and salinity was positively correlated with richness of active bacterioplankton ($\rho = 0.387$, $p = 0.007$) and benthic archaea ($\rho = 0.579$, $p = 0.003$), yet these correlations were not significant for the DNA-based richness (Fig. 7A, B). Similarly, variables significantly correlating with the DNA-based richness of planktonic bacteria (pH), planktonic archaea (temperature, DSi, NO_2^- and SRP: DSi), planktonic microeukaryotes (transparency, pH, and NO_2^-), and benthic archaea (SRP) were found to be insignificant for the active ones ($p > 0.05$; Fig. 7A, B), likely because these factors were significantly correlated with the richness of the dormant and/or the dead fractions ($p \le 0.05$; Fig. 7A, B). Significant environmental drivers for the richness of active benthic bacteria (temperature, SRP, NO_2^-, and SRP: DSi) and active benthic microeukaryotes (SRP, and SRP: DSi) were not applicable for the DNA-based richness ($p > 0.05$; Fig. 7A, B).

For dormant and dead fractions, temperature ($\rho < 0$), DSi ($\rho < 0$), DIN: DSi ($\rho > 0$), and SRP: DSi ($\rho > 0$) were often significant major drivers for the richness of in the water column ($p < 0.05$; Fig. 7A, B). Furthermore, higher levels of NH_4^+ ($\rho = 0.379$) and DIN ($\rho = 0.321$) coincided with higher richness of dormant bacterioplankton ($p < 0.05$; Fig. 7A). Both lower water content and lower nitrate concentrations were associated with a higher richness of dormant microeukaryotes in the sediments (Fig. 7B).

In explaining the variation in the assemblage structure, temperature was often found to be the strongest factor for all active, dormant, and dead microbes in both water and sediment, as well as those characterized using total DNA (Fig. 8A–W). However, more variables, especially nutrients, pH, and transparency, were identified as significant in correlation with the assemblage structure of active microbes, explaining higher proportions of variability (Fig. 8A, B, E, F, I, and J). Similar results were obtained for benthic microbes, with active ones seemingly driven by different sets of variables (Fig. 8M, N, Q, R, T, and U).

The CCA and RDA plots showed that the variations in assemblage structures of dormant and dead forms were generally poorly explained by the environmental variables measured in this study (Fig. 8, the third and fourth columns). Apart from temperature, the dormant and dead microbes were significantly correlated with various factors, including SRP: DSi, DIN: DSi, salinity, NO_2^-, NH_4^+, pH, and transparency, which, however, usually only explained < 5% of the total variations (Fig. 8C, D, K, L, P). The planktonic archaea and benthic microeukaryote assemblages in dormant forms were relatively better explained by temperature and salinity (24.5%, $p < 0.05$) and DIN: SRP (18.5%, $p < 0.05$) (Fig. 8G, V).

Discussion

Our study, using the triple metabarcoding approach (TMA), unveils for the first time the physiologically based diversity and assemblage structure of microbes across three domains, their seasonal variations, and the distinctions between water columns and surface sediments in a coastal system. We have demonstrated that there are significant proportions of dormant and dead fractions in both planktonic and sedimentary DNA pools of these microbes. Utilizing TMA to differentiate between active and dormant states of viable cells at the ASV level has yielded intriguing insights into the dormant microbes, or the “microbial seed bank”, which holds substantial ecological and evolutionary significance[11]. Our findings provide evidence that bacteria, archaea, and microeukaryotes in a dormant state are phylogenetically widespread and exhibit a diversity that surpasses previous understanding grained through enrichment techniques. Additionally, we have shown that dormant assemblages are highly dynamic, exhibiting distinct seasonality and niche specialization between water and sediment environments. Furthermore, we have discovered that extracellular DNA pools originate from different microbial sources, exhibit unique dynamics, and are influenced by various environmental factors in both water column and sediment realms.

It was estimated that DNA passing through a membrane filter (dissolved DNA) constitutes approximately 30% of total DNA pool in nearshore and estuarine waters[32]. Of the particulate DNA captured on the 0.2 μm-pore-sized polycarbonate membrane, only a minor portion (about 5%) of dead

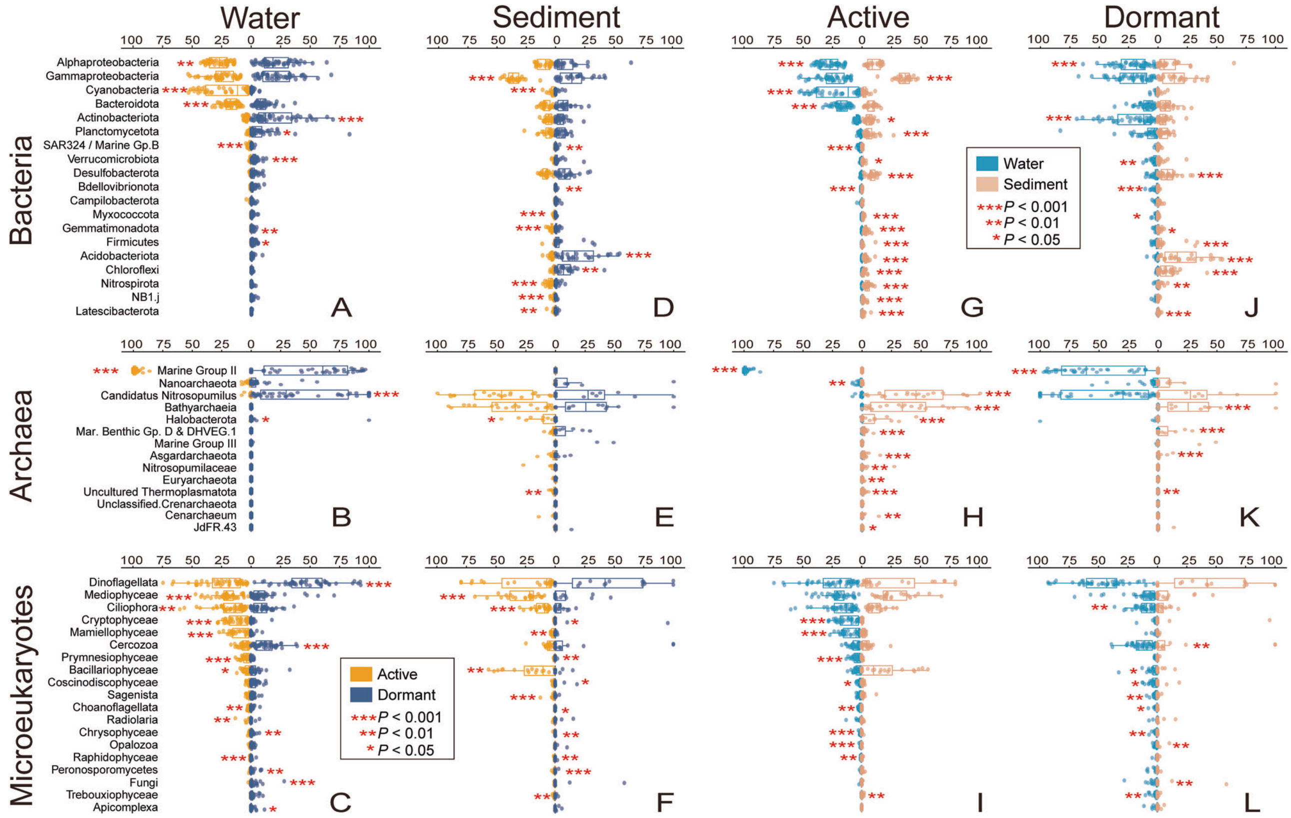

Fig. 4 | Comparisons of major microbial taxa across metabolic states and habitats. Box plots contrast the relative abundances of key bacterial (**A**, **D**, **G**, **J**), archaeal (**B**, **E**, **H**, **K**), and microeukaryotic (**C**, **F**, **I**, **L**) lineages between active and dormant assemblages (**A**–**F**) and between water and sediment (**G**–**L**) (*n* = 48 and *n* = 24 for water and sediment samples respectively, biologically independent samples).

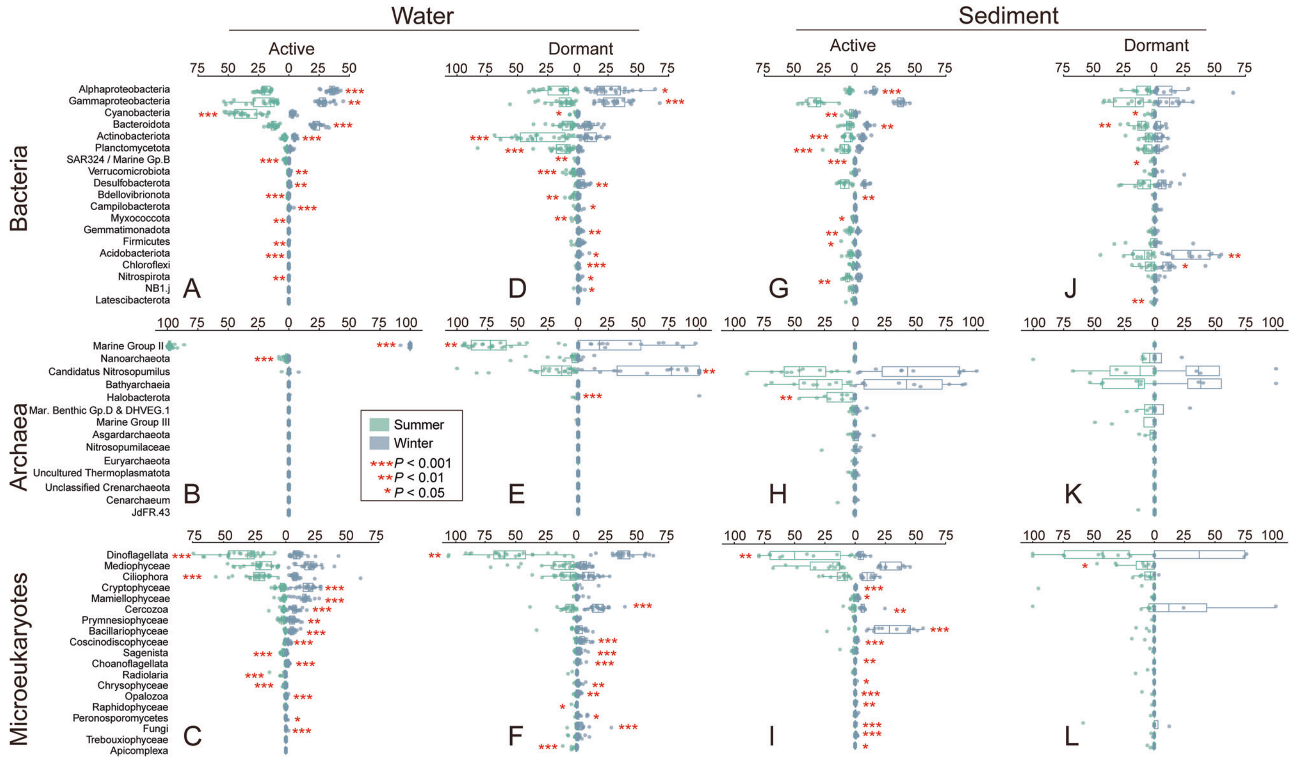

Fig. 5 | Seasonal dynamics of dominant microbial taxa across active and dormant assemblages. Box plots track the relative abundances of major lineages within active (**A**–**C**, **G**–**I**) and dormant (**D**–**F**, **J**–**L**) assemblages of bacteria (**A**, **D**, **G**, **J**), archaea (**B**, **E**, **H**, **K**), microeukaryotes (**C**, **F**, **I**, **L**) in water (**A**–**F**) and sediment (**G**–**L**) (*n* = 24 and *n* = 12 for water and sediment samples respectively, biologically independent samples).

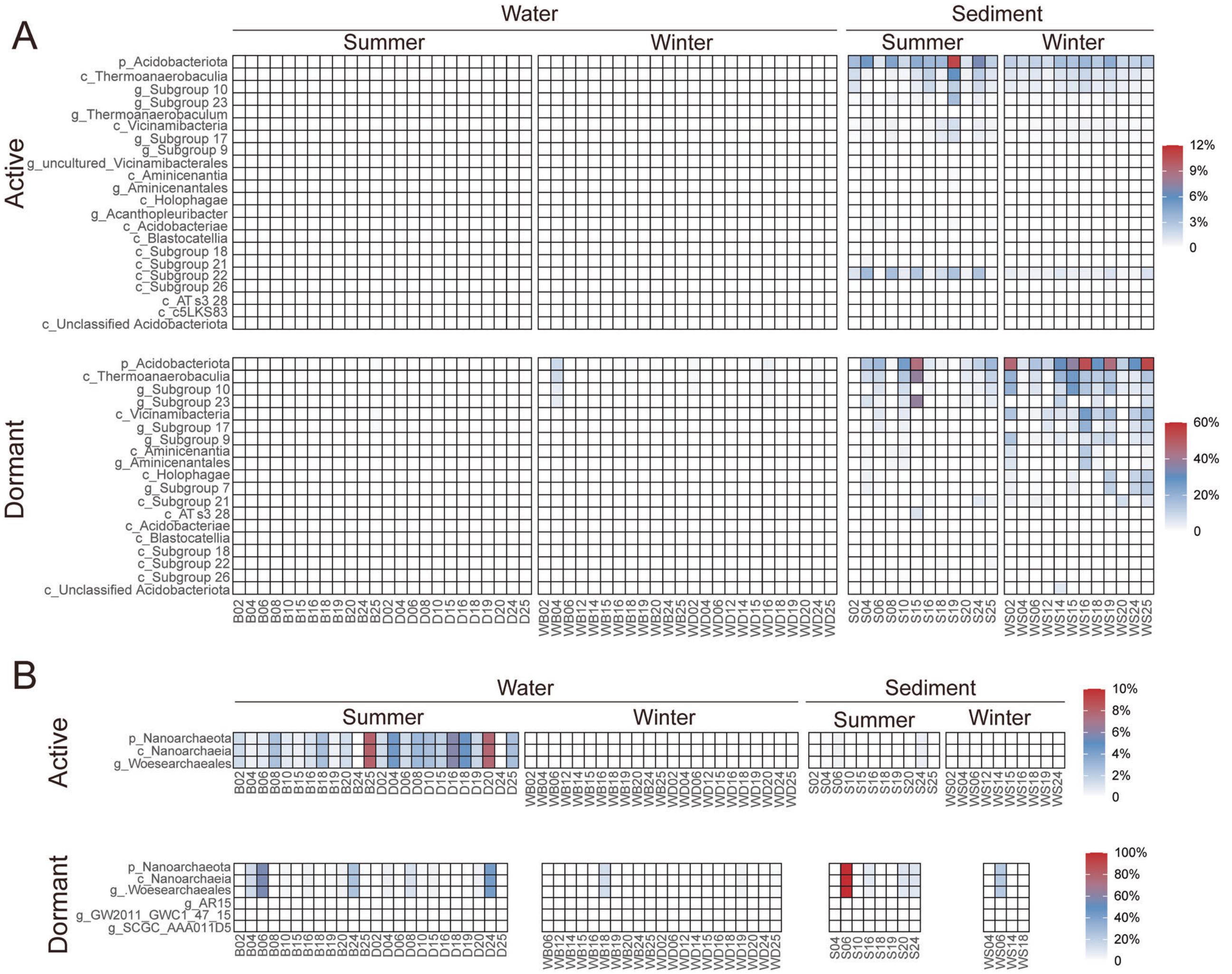

Fig. 6 | Seasonal shifts in sequence proportions of major taxa within active and dormant bacterial and archaeal assemblages. Heatmaps display the proportional representation of key lineages in both water and sediment habitats: **A** *Acidobacteriota*. **B** *Nanoarchaeota*.

planktonic microbial biomass persisted, suggesting that dissolved DNA represents a predominant component of extracellular DNA from microbial sources and can be effectively removed via filtration. The potential clogging of the size fraction (0.2–200 µm) on filters could bias the proportions of relic DNA and particulates. Future experiments might consider using multiple filter sizes to better capture different fractions of relic versus intact DNA. In contrast, in the DNA pool of surface sediments of the shallow coastal region, the dead fractions were estimated to exceed 40%, regardless of whether they were bacteria, archaea, or microeukaryotes. This could be attributed to the more rapid degradation of extracellular DNA in seawater compared to marine sediments (turnover time of 10 h vs. 29 to 93 days[33]), and the protection from nucleases of DNA absorbed onto the sediment matrix[5]. The sequence proportion of dead microeukaryotic benthos in this study is significantly higher than that found in muddy and sandy sediments of a tidal zone (14%[26]). Permanent submersion in an anoxic condition, as opposed to periodic exposure in air and oxygen penetration into deeper layers in intertidal sediments, could reduce oxidation and increase the turnover time of extracellular DNA[5], resulting in a relatively higher retention of relic DNA in the sedimentary DNA pools observed in this study.

pH was identified as the most significant factors explaining the richness and sequence proportions of physiologically distinct microbes in the rDNA pools (Fig. 1L, N), particularly for bacterioplankton and microeukaryotic plankton. These groups displayed a richer and larger active fraction and a less diverse and smaller dead fraction in summertime bottom waters and under lower pH conditions (Figs. 1C, E and S4A, C). Liang and Keeley previously demonstrated that a lower pH enhanced the recovery of extracellular DNA on filter membranes[34]. This technical aspect of pH is unlikely to account for the contrasting results we observed. Instead, biologically mediated processes, such as an increase in positively charged hydrolytic enzymes at lower pH levels, accelerate the degradation of extracellular DNA[35,36]. Moreover, pH was found to inversely co-varied with NO_2^- in our study. The accumulation of NO_2^- in bottom waters typically coincides with lower dissolved oxygen, which may inhibit the active secretion of DNA by living cells and promote passive release following cell death and cell lysis due to grazing pressure from heterotrophic protists and zooplankton[10,37]. These underlying processes could explain the higher richness proportion of dead microbes (relic DNA) in surface waters compared to bottom waters. Apart from the higher pH, the bottom water in the studied region also had lower temperatures in winter, which may contribute to a higher richness proportion of dead fractions of bacteria and microeukaryotes, as warmer temperatures facilitate degradation of extracellular DNA[35]. Coastal hypoxia is becoming increasingly prevalent, and oceanic oxygen minimum zones are expanding. Both of these phenomena can have significant impacts on microbial ecology and biogeochemical processes[38,39]. The ecophysiological adaptations of microbes in these low-oxygen and low-pH systems are fascinating topics that warrant further exploration.

Discriminating active, dead, and dormant microbial cells in environmental samples has been relatively rare in microbial ecology, with one of the key challenges being the varying criteria used to define dormancy. Using fluorescent staining to target all cellular DNA, the absence of a visible

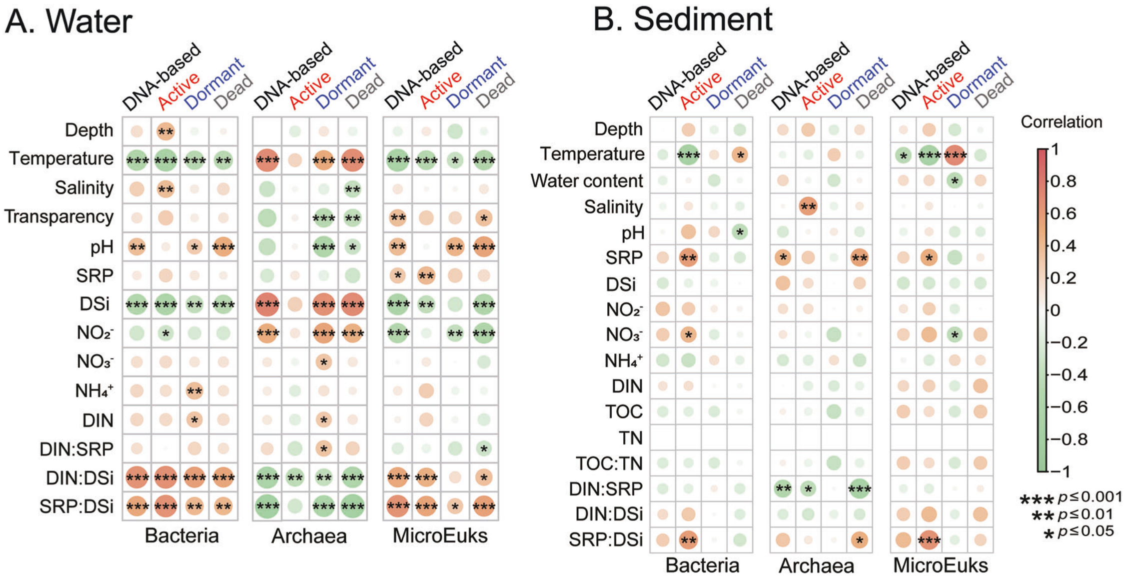

Fig. 7 | Correlations between environmental variables and the microbial diversity of physiologically distinct versus total DNA-defined microbial communities. Spearman's correlation coefficients relate environmental factors with ASV richness of the active, dormant, dead assemblages as well as of the bulk environmental DNA pool in water (**A**) and sediment (**B**) ($n = 48$ and $n = 24$ respectively, biologically independent samples). Note that the factors significantly shape traditional DNA-based richness differ markedly from those governing the active and dormant assemblages revealed by the triple metabarcoding framework. Red and green denote positive and negative correlations, respectively. DSi dissolved silicate, SRP soluble reactive phosphorus, MicroEuks microeukaryotes.

nucleoid region, and large molecular probes that penetrate only dead cells, Manini and Danovaro estimated that 40%, 30%, and 30% of prokaryotic cells were active, dormant, and dead, respectively, in Italian coastal sediments[17]. In contrast, our findings indicate a higher proportion of active (51%) and dead cells (44%) in the sediments, with dormant bacteria constituting a smaller fraction of the total rDNA pools (on average 5%). Several factors may contribute to these discrepancies. Firstly, regarding methodological differences, the rRNA gene sequence-based TMA is susceptible to variations in gene copy numbers among bacterial species and strains[40]. This implies that identical cell counts may possess varying gene copy numbers. Secondly, dormant population definition: in our analysis of triple metabarcoding data, we categorized dormant populations as those with intact cell membranes but no transcriptional activity[26]. This criterion is stringent, identifying truly dormant cells but may also bias against those that have entered dormancy yet still retain a low abundance of rRNA transcripts[41]. Thirdly, the cells on filter membranes could be stressed, physiologically altered, and physically damaged, especially when the filtration of turbid water samples becomes quickly saturated. Fourthly, different geological locations of the studied area may lead to variations in the physiological performance of microbes[42], which could account for the observed differences.

Copiotrophic bacteria typically maintain multiple rRNA gene copies in their genomes and grow rapidly, whereas oligotrophs tend to encode fewer rRNA gene copies and exhibit relatively slower growth rate compared to copiotrophs[15,43]. Given that bacterial rRNA transcript copies are generally positively correlated with rRNA gene copies[14], and oligotrophs are expected to have fewer ribosomes (and thus fewer rRNA transcripts) than copiotrophs[15], it is plausible to suspect that the TMA approach might classify oligotrophic microbes, which typically have low cellular RNA abundance, as dormant, and copiotrophs as active. To address this concern, we compared the ASV numbers of oligotrophs and copiotrophs in both dormant and active assemblages (Supplementary Fig. 8) and across major taxa (Supplementary Table 4).

In the water column, the richness of dormant oligotrophic bacteria was comparable to that of dormant copiotrophic bacteria ($p = 0.585$, $n = 48$). In contrast, in sediments, the richness of oligotrophic bacteria in dormant assemblages was significantly higher than that of copiotrophic bacteria ($p = 0.039$, $n = 24$). However, active oligotrophic bacteria also exhibited higher richness than copiotrophic bacteria in sediments ($p = 0.001$, $n = 24$). For archaea, oligotrophs generally dominated in both active and dormant assemblages ($p < 0.05$), and the richness of dormant oligotrophs and copiotrophs in sediments was not significantly different ($p = 0.08$; Supplementary Fig. 8).

Some taxa, such as *Acidobacteriota*, *Chloroflexi*, *Verrucomicrobiota*, *Planctomycetota*, and *Gemmatimonadota* are known to be slow-growing and putatively dormant (low RNA-containing) microbes in soils[44]. Our analysis indicated that most of these taxa, classified as dormant in this study, indeed belonged to oligotrophs. However, their oligotrophic phylotypes were significantly richer than copiotrophic ones in active assemblages, regardless of whether they were in water or sediment (Supplementary Table 4). Furthermore, both active and dormant phylotypes of the well-known oligotrophic bacterial group SAR11 were consistently more represented by copiotrophic rather than oligotrophic ones (Supplementary Table 4). Therefore, we conclude that there is insufficient evidence to support the notion that dormancy and activity in prokaryotes identified in this study are strongly correlated with their trophic strategies.

Consistent with our previous study that revealed a considerable diversity but a low sequence proportion of dormant microeukaryotes in intertidal sediments[26], the current study extends these findings to bacteria and archaea in both planktonic and benthic environments. Both studies support the concept that most dormant microbes are rare within the communities, acting as a genetic diversity reservoir in the studied systems[14,45]. The high diversity of dormant populations also suggests that the alpha diversity of active or functional microbes may have been overestimated in many traditional DNA-based metabarcoding studies[46], and the recent metabarcoding of PMA-treated DNA targeting viable populations[6].

Our study identified some dormant bacterial taxa that were also recognized through lysis and enrichments in previous studies, highlighting the effectiveness of TMA in recovering dormant taxa from the environment. For instance, after physical and chemical lysis, spore-forming bacteria in sediments and human fecal samples were enriched and mostly identified as the endospores or exospore of *Firmicutes*, sulfate-reducing bacteria, and *Actinobacteria*[13,19,20,47,48]. These taxa were also found to be abundant as dormant members in the present study. Furthermore, our results on

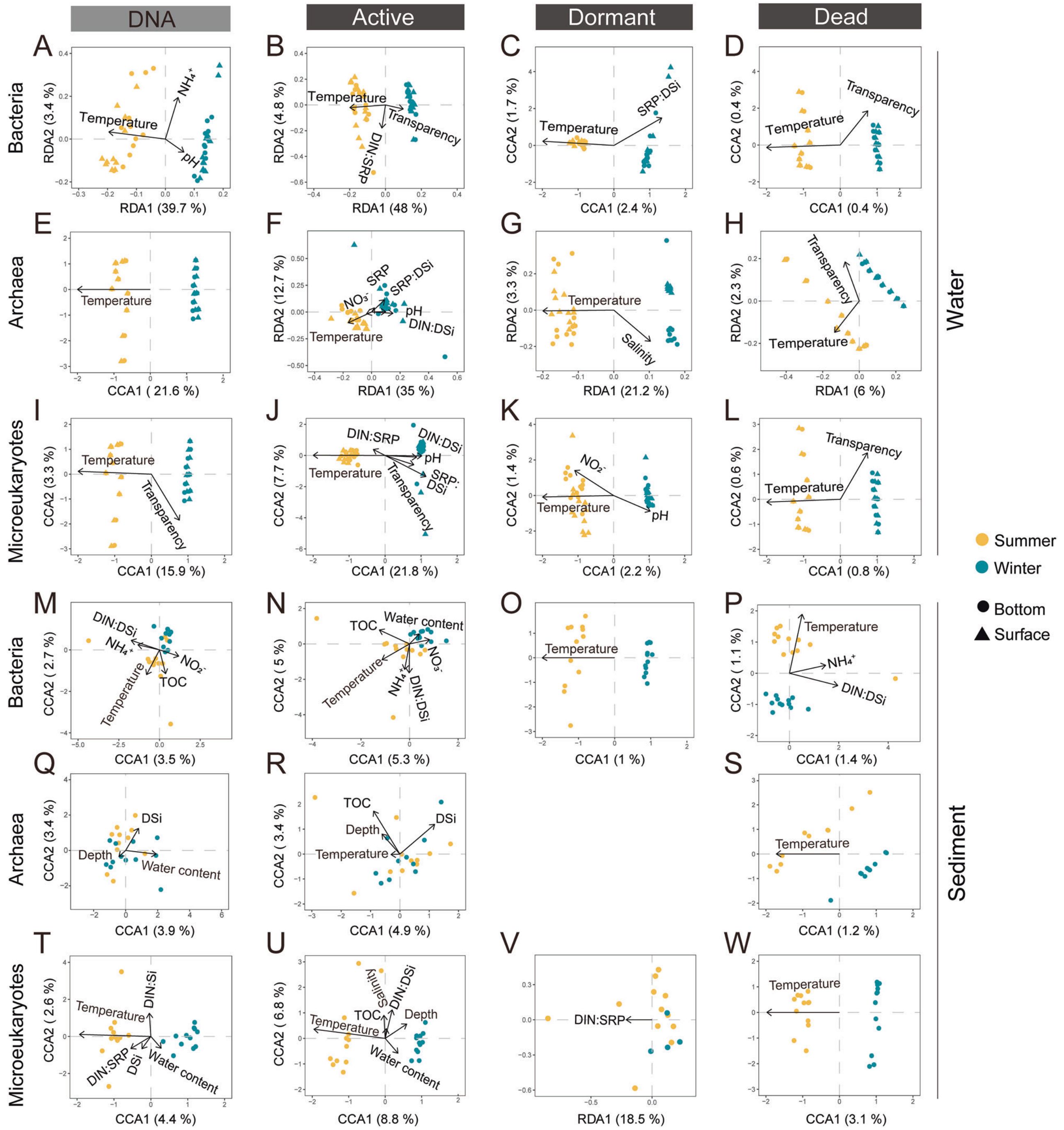

Fig. 8 | Comparisons of key environmental factors explaining the variations in assemblage structures of physiologically distinct microbes and of the total rDNA pool. Plots of canonical correspondence analysis (CCA) or redundancy analysis (RDA) showing the most influential environmental factors in relation to assemblage structures of bacteria (**B**–**C**, **N**–**P**), archaea (**F**–**H**, **Q**–**S**), microeukaryotes (**I**–**L**, **T**–**W**) of different physiological states, and of the environmental DNA-based (leftmost column), in waters (**A**–**L**) and sediments (**M**–**W**). Note that the factors best explain the variations in traditionally DNA-based communities differ markedly from those governing the active and dormant fractions resolved by the triple metabarcoding approach. DSi dissolved silicate, SRP soluble reactive phosphorus.

dormant taxa in surface sediments align with Corona Ramírez et al.[48] who demonstrated that many members of *Proteobacteria* and *Chloroflexi* were abundant in lysis-resistant assemblages in lake sediments.

In our examination of sediments, *Acidobacteriota* appeared dominant in dormant assemblages (22%) but were rare in active assemblages (3%) (Fig. 4J). This finding contrasts with previous studies, in which dormant *Acidobacteriota* were barely detected using lysis-resistant methods[19,48]. The vast majority of *Acidobacteria* remain uncultured, whereas 16S rDNA-based surveys have shown this phylum to be abundant across diverse habitats, particularly in soils. All cultured species were thought to be oligotrophic and non-spore forming, and recent studies showed that genomes of acidobacterial representatives contain H_2-uptake [NiFe]-hydrogenase and many physiology-relevant genes that enable them to adapt to stress and starvation[44,49]. Despite of these advances, knowledge of their ecophysiology in various ecosystems is limited[49]. Our finding provides the first community-level evidence for the importance of *Acidobacteria* in the bacterial seed bank, and the dormancy of various lineages of *Acidobacteria* members in the environment warrants further investigation to better understand their physiology and ecology across different environments and times.

Taxonomic distribution of dormant bacteria and archaea in plankton has been molecularly assessed using rRNA to rDNA ratio as an indicator (e.g.,[14–16]. However, these studies have rarely taken extracellular DNA and dead cells into account. After pasteurization and incubation, the thermophilic fermentative endospores of *Firmicutes* in coastal waters underwent germination and were subsequently identified and enumerated[50]. In our study, the spore-forming *Firmicutes* (1.1%) and *Desulfobacterota* (1.8%) were found to be minor components of the dormant bacterioplankton assemblage (Fig. 4A and Supplementary Table 3). We found a high contribution of *Actinobacteriota* (20%) to the dormant bacterioplankton in the river plume region (Fig. 4A and Supplementary Table 3), aligning with the notion that many actinobacterial spores are washed into and survive for long periods in freshwater and marine habitats[51]. Furthermore, the dominance of *Gamma*- (22%) and *Alphaproteobacteria* (21%), and the abundance of *Bacteriodota*, *Planctomycetota*, and *Verrucomicrobiota* in the dormant bacterioplankton assemblage was seldomly reported (Fig. 4A and Supplementary Table 3). This may be because not all microbes enter dormant state by forming spores[48], and some taxa might be destroyed or damaged by physical and chemical treatments during enrichment.

Dormancy has been sporadically reported for halophilic and thermophilic archaeal species[52–55]. Lysis-resistant archaea enriched from polyextreme benthos were identified to be mainly *Halobacteria* and *Thaumarchaeota* (or ammonia-oxidizing archaea, AOA)[48], which were also recovered as dormant members in our study. Additionally, two archaeal groups, *Bathyarchaeia*, known as important degraders of organic matter in sediments[56], Ca. *Nitrosopumilus*, well-known ammonia oxidizers[57], were found to be abundant in both the dormant and active archaeal assemblages in the benthos. This suggests physiological specialization within these two groups, indicating that not all co-occurring phylotypes are actively functioning in the surface sediments. In the water columns, viable cells of Ca. *Nitrosopumilus* were detectable but appeared to be completely inactive, possibly due to photoinhibition of AOA activity in sunlight-exposed shallow waters[58]. *Nanoarchaeota*, putative obligate archaeal symbionts[59], were mostly dormant in both sediments and waters, a new finding that demonstrates much remains to be discovered about their activity and ecological role in marine systems. It was not surprising that Marine Group II was active in the coastal water columns, as they are likely photoheterotrophs and frequently positively correlated with phytoplankton biomass[60]. These results highlight that dormancy may be a physiological factor affecting biogeochemical and ecological activity of these archaea in the marine environment.

Resting cysts of relatively large cell-sized ciliates and dinoflagellates in sediments have been documented[61,62]. In our study of dormant microeukaryotes, dinoflagellates (richness% < 38% and seq% < 50%) and ciliates (richness% < 11% and seq% < 11%) were indeed among the most diverse and dominant. Nevertheless, the dormant phenotypes of many taxa, which were rarely quantified in environmental studies, were found with moderate sequence proportions in the dormancy assemblages of both water columns and sediments (e.g., *Cercozoa* < 16%; *Mediophyceae* < 11%; *Cryptophyceae* < 7%). Cysts of these protistan taxa have been documented[63–65].

Our study revealed that the environmental factors driving the richness and community structure of active microbes differ from those based on total DNA, suggesting that including dormant and dead microbes in metabarcoding data could lead to incorrect inferences about the anthropogenic and climatic impacts on microbial structure and function. In a stable system, where the total species number across different physiological states remains constant, we hypothesize that environmental stress-induced physiological shifts would result in factors promoting active microbial richness inversely correlating with those of dormant and dead microbes. This hypothesis appears to hold true for benthic bacteria and microeukaryotes in this study (Fig. 7B), and our previous microcosm incubation investigation of benthic microeukaryotes[26], but not for planktonic microbes. Here, colder temperatures and lower concentrations of DSi promoted the richness of active, dormant, and dead microbes alike (Fig. 7A). These discrepancies can be attributed to the differences in species pool size and stability between water and sediment. Pelagic systems are dynamic and resource-dependent, with currents and flows bringing species into and out of the studied area. The number of dormant and dead species is largely dependent on the pool size of active species, which is partly driven by DSi, a nutrient essential for diatom production. In contrast, sediment species pools are more stable, with limited species dispersal; thus, a higher number of active species is achieved at the cost of reactivating dormant ones.

Conclusion

Our study supports the notion that active microbes are predominantly abundant within the communities, while dormant forms are relatively rare and deceased microbes are pervasive across natural environments. This study also underscores the dynamic nature of dormant assemblages, which exhibit clear seasonality and niche-specific adaptations. Our findings reveal substantial representation of both dormant and dead microbes in the whole DNA pools extracted from environmental samples, challenging the conventional metabarcoding assessments that may overestimate the active microbial diversity of bacteria, archaea, and microeukaryotes. However, the environmental factors we measured explain very little of the variation observed in the assemblages of dormant and dead microbes. In this study, we did not measure other chemical stressors such as antibiotics, heavy metals, and organic pollutants, which are known to trigger microbial dormancy[59]. Diel variations in microbial metabolic activity and gene expression have been shown to be distinct in water columns[14,66,67]. The impact of diel rhythms on microbial eco-physiological states remains to be examined. We did not consider dispersal processes such as sedimentation from pelagic to benthic environments and re-suspension from benthic to pelagic, were not included in this study. However, these processes could play a role in driving microbial succession, physiological changes, and die-off. Furthermore, biotic interactions such as predation, competition, allelopathy, parasitism, and mutualism have been suggested as significant factors in explaining the unresolved variability in DNA-based microbial diversity[67,68]. We further posit that biotic interactions could substantially influence microbial ecophysiology and biogeography. Additional investigation into these factors is essential to unravel the intricate effects and interactions that shape the ecophysiology-based diversity of microbes across various ecosystems.

Methods

Sampling

The sampling area was situated in the estuarine plume area of the northern Beibu Gulf, to the west of the Leizhou Peninsula and the northern South China Sea (Supplementary Fig. 9). During two expeditions in August 2023 (12 stations) and January 2024 (12 stations), surface (at a depth of 0.5 m) and bottom water samples (1 m above the seafloor) were collected using a portable water sampler. Meanwhile, sediment samples were gathered with a Van Veen grab sampler (Hydro-Bios), and the top 1-cm layers were subsampled with a custom-made corer (inner diameter 1.5 cm). Sampling took place from 08:00 to 16:00 each day. In situ measurements of water temperature, pH, and salinity were conducted using a pH meter (Testo, Pennsylvania, USA) and a salinity meter (Vastocean, Shanghai, China).

The water samples were first pre-filtered through a 200-μm mesh to remove large particles, and then 1 liter of the filtrate was further filtered through a 0.2-μm-pore-sized polycarbonate membrane (47 mm diameter; Millipore, Germany) to capture microbial biomass. Both the membranes with the retained biomass and the sediment samples were stored at −80 °C for subsequent nucleic acid extraction. The filtrate was kept at −20 °C for nutrient analysis.

Determination of physicochemical variables

Sediment subsamples were freeze-dried using a vacuum freezer (Boyikang, Beijing) to achieve a constant weight, which allowed for the calculation of water content. Total organic carbon (TOC) and total nitrogen (TN) were determined using an elemental analyzer (Elementar Macrocube, Germany). Additional sediment subsamples were mixed with distilled water at a 1:2.5

ratio, and their pH and salinity were measured using the same methods as for seawater samples. Nutrients in the sediment were extracted with 2 M KCl solution, and the concentrations of nitrate (NO_3^-), nitrite (NO_2^-), ammonium (NH_4^+), soluble reactive phosphate (SRP), and dissolved silicate (DSi) in both the extracted solution and the seawater were analyzed using a flow auto-analyzer (Technicon AA3, Bran-Lubbe, Norderstedt, Germany). For summary of environmental variables, see Supplementary Table 5.

PMA treatment, nucleic acid extraction, and reverse transcription

The PMA treatment for sediment samples followed previously published protocols[6,26]. Specifically, two aliquots of each sediment sample were resuspended in 8 mL PBS (pH 7.2–7.4) in transparent polystyrene tubes (Falcon, USA) and gently mixed with PMAxx (Biotium, USA) to achieve a final concentration of 40 μM. The samples were then incubated for 4 min in the dark. Subsequently, the tubes were exposed to a 650 W halogen lamp for four 30:30 s light:dark cycles. The PMA-treated samples were filtered onto 0.2-μm-pore-sized membrane filters (Millipore, Germany) for subsequent DNA extraction. For seawater samples, the PMA treatment was carried out as previously described[23,69], with modifications (Supplementary Fig. 10). In brief, 500 ml of seawater was added to the holding cup, passing through a 0.2-μm-pore-sized polycarbonate membrane, leaving 5–10 ml of water in the cup. A PMAxx solution (final concentration of 40 μM) was then added and incubated in the dark for 10 min. Light activation and final filtration were performed as described. All filters were stored at −80 °C until DNA extraction using the PowerSoil Kit (QIAGEN, Germany). Co-extraction of DNA and RNA and reverse transcription were conducted as detailed by Deng et al.[26].

High through sequencing and data processing

The V4 hypervariable region of the 16S rRNA and 18S rRNA gene were amplified using universal primers 515F (5′-GTGYCAGCMGCCGCGGTAA-3′)[70] and 806R (5′-GGACTACNVGGGTWTCTAAT-3′)[71] for bacteria, Arch519f (5′-CAGCCGCCGCGGTAA-3′) and Arch915r (5′-GTGCTCCCCCGCCAATTCCT-3′) for archaea[72], and euk454F (5′-CCAGCASCYGCGGTAATTCC-3′) and UeukREV3 (5′-ACTTTCGTTCTTGAT-3′) for microeukaryotes[73]. PCR reactions were conducted with an initial denaturation at 98 °C for 1 min, followed by 30 cycles of denaturation at 98 °C for 10 s, annealing at 50 °C for 30 s, and elongation at 72 °C for 30 s and 72 °C for 5 min. PCR products were purified with Universal DNA Purification Kit (TianGen, China), and sequencing libraries were generated using NEB Next Ultra II FS DNA PCR-Free Library Prep Kit (New England Biolabs, USA). Sequencing was performed on an Illumina Novaseq 6000 PE250 platform at a commercial company (Novogene, China).

Sequence data were processed using QIIME 2 version 2021.4[74]. Raw reads were imported into QIIME 2 using the q2-import plugin and demultiplexed using the q2-demux plugin. ASVs were generated and filtered for quality using DADA2 through the q2-dada2 plugin (Supplementary Data 4). Microbial taxonomy was assigned to ASVs using a naive Bayes classifier trained on the SILVA database (Release 138.1) for bacteria and archaea, and the PR2 database (Version 5.0.0) for microeukaryotes. Active, dormant, and dead ASVs were categorized based on sequence datasets obtained from DNA-seq, RNA-seq, and PMA-seq using a custom script (https://github.com/vivenha/) and under the following criterion[26]: (1) the PMA-seq covers the ASVs of cell membrane-intact components (e.g., dormant and active ASVs); (2) the ASVs detected in both the DNA-seq and RNA-seq are considered to be active; (3) the ASVs observed in the DNA-seq but neither in PMA-seq nor RNA-seq dataset are considered dead; (4) those detected in PMA-seq and/or RNA-seq but not present in DNA-seq are the theoretically absent (T-absent) ASVs, which may reflect either methodological issues or lack of sufficient sequencing depth. Sequence counts of the ASVs in active assemblages were retrieved from RNA-seq data, because rRNA transcript copy numbers reflect the biomass of protistan cells better than rDNA[28]. Sequence counts of the ASVs in dormant and dead assemblages were obtained from PMA-seq and DNA-seq data, respectively[26] (Supplementary Fig. 11). The sequences of three components (active, dormant, and dead) were rarefied to the minimum sample sequence number within each component, and subsequent analyses of alpha and beta diversities were conducted using the rarefied data.

Statistics and reproducibility

All data analyses and visualizations were conducted using *R* (ver. 4.3.2). Alpha diversity estimators (ASV richness, Chao1, Shannon, and Simpson indices) were calculated using *vegan* (ver. 2.5–7). To assess the differences in microbial alpha diversity estimators, sequence proportions, environmental factors, and major taxa across various niches (surface, bottom waters, and sediments) and seasons (summer and winter), we utilized one-way analysis of variance (ANOVA) and Mann–Whitney *U* test. Community structure was evaluated based on Bray-Curtis dissimilarities, with variations visualized through non-metric multidimensional scaling (NMDS). The null hypotheses that there were no differences in community structure among niches and between seasons were tested using analysis of similarity (ANOSIM). Canonical correspondence analysis (CCA) and redundancy analysis (RDA) were performed to investigate the relationships between community structure and environmental factors. Additionally, Spearman's rank correlation analysis was conducted to explore the correlations between ASV richness, the sequence proportions of different taxa, and environmental factors.

Reporting summary

Further information on research design is available in the Nature Portfolio Reporting Summary linked to this article.

Data availability

The datasets supporting the conclusions of this article are available in the National Center for Biotechnology Information (NCBI) repository, PRJNA1202647 for bacteria (https://www.ncbi.nlm.nih.gov/bioproject/PRJNA1202647), PRJNA1203040 for archaea (https://www.ncbi.nlm.nih.gov/bioproject/PRJNA1203040), and PRJNA1203028 for microeukaryotes (https://www.ncbi.nlm.nih.gov/bioproject/PRJNA1203028). All data is available for download. The data underlying Figs. 1–8 can be found in Supplementary Data 5.

Code availability

The R codes used in this study were available on GitHub (https://github.com/vivenha/).

Received: 4 February 2025; Accepted: 25 August 2025;

References

1. Giner, C. R. et al. Marked changes in diversity and relative activity of picoeukaryotes with depth in the world ocean. *ISME J.* **14**, 437–449 (2020).
2. Salazar, G. & Sunagawa, S. Marine microbial diversity. *Curr. Biol.* **27**, R489–R494 (2017).
3. Zinger, L., Gobet, A. & Pommier, T. Two decades of describing the unseen majority of aquatic microbial diversity. *Mol. Ecol.* **21**, 1878–1896 (2012).
4. Dell'Anno, A. & Danovaro, R. Extracellular DNA plays a key role in deep-sea ecosystem functioning. *Science* **309**, 2179–2179 (2005).
5. Torti, A., Lever, M. A. & Jørgensen, B. B. Origin, dynamics, and implications of extracellular DNA pools in marine sediments. *Mar. Genom.* **24**, 185–196 (2015).
6. Carini, P. et al. Relic DNA is abundant in soil and obscures estimates of soil microbial diversity. *Nat. Microbiol.* **2**, 1–6 (2016).
7. Checinska, A. et al. Microbiomes of the dust particles collected from the International Space Station and Spacecraft Assembly Facilities. *Microbiome* **3**, 1–18 (2015).

8. Ni, J., Hatori, S., Wang, Y., Li, Y.-Y. & Kubota, K. Uncovering viable microbiome in anaerobic sludge digesters by propidium monoazide (PMA)-PCR. *Microb. Ecol.* **79**, 925–932 (2020).
9. Luna, G., Manini, E. & Danovaro, R. Large fraction of dead and inactive bacteria in coastal marine sediments: comparison of protocols for determination and ecological significance. *Appl. Environ. Microbiol.* **68**, 3509–3513 (2002).
10. Nielsen, K. M., Johnsen, P. J., Bensasson, D. & Daffonchio, D. Release and persistence of extracellular DNA in the environment. *Environ. Biosaf. Res.* **6**, 37–53 (2007).
11. Jones, S. E. & Lennon, J. T. Dormancy contributes to the maintenance of microbial diversity. *Proc. Natl. Acad. Sci. USA* **107**, 5881–5886 (2010).
12. Blagodatskaya, E. & Kuzyakov, Y. Active microorganisms in soil: critical review of estimation criteria and approaches. *Soil Biol. Biochem.* **67**, 192–211 (2013).
13. Burkert, A., Douglas, T. A., Waldrop, M. P. & Mackelprang, R. Changes in the active, dead, and dormant microbial community structure across a Pleistocene permafrost chronosequence. *Appl. Environ. Microbiol.* **85**, e02646–02618 (2019).
14. Campbell, B. J., Yu, L., Heidelberg, J. F. & Kirchman, D. L. Activity of abundant and rare bacteria in a coastal ocean. *Proc. Natl. Acad. Sci. USA* **108**, 12776–12781 (2011).
15. Kirchman, D. L. Growth rates of microbes in the oceans. *Ann. Rev. Mar. Sci.* **8**, 285–309 (2016).
16. Lankiewicz, T. S., Cottrell, M. T. & Kirchman, D. L. Growth rates and rRNA content of four marine bacteria in pure cultures and in the Delaware estuary. *ISME J.* **10**, 823–832 (2016).
17. Manini, E. & Danovaro, R. Synoptic determination of living/dead and active/dormant bacterial fractions in marine sediments. *FEMS Microbiol. Ecol.* **55**, 416–423 (2006).
18. Sisson, C., Gulla-Devaney, B., Katz, L. A. & Grattepanche, J.-D. Seed bank and seasonal patterns of the eukaryotic SAR (Stramenopila, Alveolata and Rhizaria) clade in a New England vernal pool. *J. Plankton Res.* **40**, 376–390 (2018).
19. Wunderlin, T., Junier, T., Roussel-Delif, L., Jeanneret, N. & Junier, P. Endospore-enriched sequencing approach reveals unprecedented diversity of F irmicutes in sediments. *Environ. Microbiol. Rep.* **6**, 631–639 (2014).
20. de Rezende, J. R., Hubert, C. R., Røy, H., Kjeldsen, K. U. & Jørgensen, B. B. Estimating the abundance of endospores of sulfate-reducing bacteria in environmental samples by inducing germination and exponential growth. *Geomicrobiol. J.* **34**, 338–345 (2017).
21. Lindivat, M., Larsen, A., Hess-Erga, O. K., Bratbak, G. & Hoell, I. A. Bioorthogonal non-canonical amino acid tagging combined with flow cytometry for determination of activity in aquatic microorganisms. *Front. Microbiol.* **11**, 1929 (2020).
22. Nocker, A., Sossa-Fernandez, P., Burr, M. D. & Camper, A. K. Use of propidium monoazide for live/dead distinction in microbial ecology. *Appl. Environ. Microbiol.* **73**, 5111–5117 (2007).
23. Nocker, A., Richter-Heitmann, T., Montijn, R., Schuren, F. & Kort, R. Discrimination between live and dead cells in bacterial communities from environmental water samples analyzed by 454 pyrosequencing. *Int. Microbiol.* **13**, 59–65 (2010).
24. Vaishampayan, P. et al. New perspectives on viable microbial communities in low-biomass cleanroom environments. *ISME J.* **7**, 312–324 (2013).
25. Emerson, J. B. et al. Schrödinger's microbes: tools for distinguishing the living from the dead in microbial ecosystems. *Microbiome* **5**, 1–23 (2017).
26. Deng, H., He, C., Worden, A. Z. & Gong, J. Employing a triple metabarcoding approach to differentiate active, dormant and dead microeukaryotes in sediments. *Environ. Microbiol.* **26**, e16615 (2024).
27. Fu, R. & Gong, J. Single cell analysis linking ribosomal (r) DNA and rRNA copy numbers to cell size and growth rate provides insights into molecular protistan ecology. *J. Eukaryot. Microbiol.* **64**, 885–896 (2017).
28. Zou, S. et al. Coupling between ribotypic and phenotypic traits of protists across life cycle stages and temperatures. *Microbiol. Spectr.* **9**, e01738–01721 (2021).
29. Steven, B., Hesse, C., Soghigian, J., Gallegos-Graves, L. V. & Dunbar, J. Simulated rRNA/DNA ratios show potential to misclassify active populations as dormant. *Appl. Environ. Microbiol.* **83**, e00696–00617 (2017).
30. Bairoliya, S., Koh Zhi Xiang, J. & Cao, B. Extracellular DNA in environmental samples: occurrence, extraction, quantification, and impact on microbial biodiversity assessment. *Appl. Environ. Microbiol.* **88**, e01845–01821 (2022).
31. Corliss, J. O. Protozoan cysts and spores in *Encyclopedia of Life Sciences* 1–8 (John Wiley & Sons, Chichester, 2001).
32. DeFlaun, M. F., Paul, J. H. & Jeffrey, W. H. Distribution and molecular weight of dissolved DNA in subtropical estuarine and oceanic environments. *Mar. Ecol. Prog. Ser.* **38**, 65 (1987).
33. Dell'Anno, A. & Corinaldesi, C. Degradation and turnover of extracellular DNA in marine sediments: ecological and methodological considerations. *Appl. Environ. Microbiol.* **70**, 4384–4386 (2004).
34. Liang, Z. & Keeley, A. Filtration recovery of extracellular DNA from environmental water samples. *Environ. Sci. Technol.* **47**, 9324–9331 (2013).
35. Strickler, K. M., Fremier, A. K. & Goldberg, C. S. Quantifying effects of UV-B, temperature, and pH on eDNA degradation in aquatic microcosms. *Biol. Conserv.* **183**, 85–92 (2015).
36. Seymour, M. et al. Acidity promotes degradation of multi-species environmental DNA in lotic mesocosms. *Commun. Biol.* **1**, 4 (2018).
37. Rocke, E. & Liu, H. Respiration, growth and grazing rates of three ciliate species in hypoxic conditions. *Mar. Pollut. Bull.* **85**, 410–417 (2014).
38. Wright, J. J., Konwar, K. M. & Hallam, S. J. Microbial ecology of expanding oxygen minimum zones. *Nat. Rev. Microbiol.* **10**, 381–394 (2012).
39. Breitburg, D. et al. Declining oxygen in the global ocean and coastal waters. *Science* **359**, eaam7240 (2018).
40. Sun, D.-L., Jiang, X., Wu, Q. L. & Zhou, N.-Y. Intragenomic heterogeneity of 16S rRNA genes causes overestimation of prokaryotic diversity. *Appl. Environ. Microbiol.* **79**, 5962–5969 (2013).
41. Segev, E., Smith, Y. & Ben-Yehuda, S. RNA dynamics in aging bacterial spores. *Cell* **148**, 139–149 (2012).
42. Louthan, A. M., DeMarche, M. L. & Shoemaker, L. G. Climate sensitivity across latitude: scaling physiology to communities. *Trends Ecol. Evol.* **36**, 931–942 (2021).
43. Roller, B. R., Stoddard, S. F. & Schmidt, T. M. Exploiting rRNA operon copy number to investigate bacterial reproductive strategies. *Nat. Microbiol.* **1**, 1–7 (2016).
44. Greening, C. et al. Persistence of the dominant soil phylum Acidobacteria by trace gas scavenging. *Proc. Natl. Acad. Sci. USA* **112**, 10497–10502 (2015).
45. Lennon, J. T. & Jones, S. E. Microbial seed banks: the ecological and evolutionary implications of dormancy. *Nat. Rev. Microbiol.* **9**, 119–130 (2011).
46. Gong, J. et al. Depth shapes α-and β-diversities of microbial eukaryotes in surficial sediments of coastal ecosystems. *Environ. Microbiol.* **17**, 3722–3737 (2015).
47. Kearney, S. M. et al. Endospores and other lysis-resistant bacteria comprise a widely shared core community within the human microbiota. *ISME J.* **12**, 2403–2416 (2018).
48. Corona Ramírez, A., Cailleau, G., Fatton, M., Dorador, C. & Junier, P. Diversity of lysis-resistant bacteria and archaea in the Polyextreme environment of Salar de Huasco. *Front. Microbiol.* **13**, 826117 (2022).
49. Kalam, S. et al. Recent understanding of soil acidobacteria and their ecological significance: a critical review. *Front. Microbiol.* **11**, 580024 (2020).

50. Volpi, M. et al. Identity, abundance, and reactivation kinetics of thermophilic fermentative endospores in cold marine sediment and seawater. *Front. Microbiol.* **8**, 131 (2017).
51. Goodfellow, M. & Williams, S. Ecology of Actinomycetes. *Ann. Rev. Microbiol.* **37**, 189 (1983).
52. Fendrihan, S. et al. Spherical particles of halophilic archaea correlate with exposure to low water activity–implications for microbial survival in fluid inclusions of ancient halite. *Geobiology* **10**, 424–433 (2012).
53. Bautista, M. A., Zhang, C. & Whitaker, R. J. Virus-induced dormancy in the archaeon Sulfolobus islandicus. *mBio* **6**, 02565–02514 (2015).
54. Mukherjee, A. et al. VapC toxins drive cellular dormancy under uranium stress for the extreme thermoacidophile Metallosphaera prunae. *Environ. Microbiol.* **19**, 2831–2842 (2017).
55. Tang, S.-K. et al. Cellular differentiation into hyphae and spores in halophilic archaea. *Nat. Commun.* **14**, 1827 (2023).
56. Yu, T. et al. Growth of sedimentary Bathyarchaeota on lignin as an energy source. *Proc. Natl. Acad. Sci. USA* **115**, 6022–6027 (2018).
57. Zheng, Y. et al. Novel order-level lineage of ammonia-oxidizing archaea widespread in marine and terrestrial environments. *ISME J.* **18**, wrad002 (2024).
58. Horak, R. E. et al. Relative impacts of light, temperature, and reactive oxygen on thaumarchaeal ammonia oxidation in the North Pacific Ocean. *Limnol. Oceanogr.* **63**, 741–757 (2018).
59. Huber, H. et al. A new phylum of Archaea represented by a nanosized hyperthermophilic symbiont. *Nature* **417**, 63–67 (2002).
60. Chen, S. et al. Interactions Between marine group II Archaea and phytoplankton revealed by population correlations in the northern coast of South China Sea. *Front. Microbiol.* **12**, 785532 (2022).
61. Esteban, G. F. & Finlay, B. J. Cryptic freshwater ciliates in a hypersaline lagoon. *Protist* **154**, 411–418 (2003).
62. Persson, A. Proliferation of cryptic protists and germination of resting stages from untreated sediment samples with emphasis on dinoflagellates. *Ophelia* **55**, 151–166 (2001).
63. Hoef-Emden, K. & Archibald, J. M. Cryptophyta (cryptomonads). *Handb. Protists* **724**, 851–891 (2017).
64. Howe, A. T., Bass, D., Vickerman, K., Chao, E. E. & Cavalier-Smith, T. Phylogeny, taxonomy, and astounding genetic diversity of Glissomonadida ord. Nov., the dominant gliding zooflagellates in soil (Protozoa: Cercozoa). *Protist* **160**, 159–189 (2009).
65. McQuoid, M. R. & Hobson, L. A. Diatom resting stages. *J. Phycol*. **32**, 889–902 (1996).
66. Zehnpfennig, J. R. et al. Diel patterns in marine microbial Metatranscriptomes reflect differences in community metabolic activity over depth on the continental shelf of the North Atlantic. *Front. Mar. Sci.* **9**, 798877 (2022).
67. He, C. et al. Spatial and diel variations of bacterioplankton and pico-nanoeukaryote communities and potential biotic interactions during macroalgal blooms. *Mar. Pollut. Bull.* **202**, 116409 (2024).
68. Li, G., Wang, Y., Li, H., Zhang, X. & Gong, J. Quantifying relative contributions of biotic interactions to bacterial diversity and community assembly by using community characteristics of microbial eukaryotes. *Ecol. Indic.* **146**, 109841 (2023).
69. Hellein, K. N. et al. A filter-based propidium monoazide technique to distinguish live from membrane-compromised microorganisms using quantitative PCR. *J. Microbiol. Methods* **89**, 76–78 (2012).
70. Parada, A. E., Needham, D. M. & Fuhrman, J. A. Every base matters: assessing small subunit rRNA primers for marine microbiomes with mock communities, time series and global field samples. *Environ. Microbiol.* **18**, 1403–1414 (2016).
71. Apprill, A., McNally, S., Parsons, R. & Weber, L. Minor revision to V4 region SSU rRNA 806R gene primer greatly increases detection of SAR11 bacterioplankton. *Aquat. Microb. Ecol.* **75**, 129–137 (2015).
72. Herfort, L. et al. Diversity of Archaea and detection of crenarchaeotal amoA genes in the rivers Rhine and Tet. *Aquat. Microb. Ecol.* **55**, 189–201 (2009).
73. Lin, Y. et al. Specific eukaryotic plankton are good predictors of net community production in the Western Antarctic Peninsula. *Sci. Rep.* **7**, 14845 (2017).
74. Bolyen, E. et al. Reproducible, interactive, scalable and extensible microbiome data science using QIIME 2. *Nat. Biotechnol.* **37**, 852–857 (2019).

Acknowledgements

This work was supported by the National Natural Science Foundation of China (No. 42376086), the Innovation Group Project of Southern Marine Science and Engineering Guangdong Laboratory (Zhuhai) (No. 311021004), the Guangdong Basic and Applied Basic Research Foundation (No. 2022A1515240020), and the Implementing the Strategic Action Program for the South China Sea and Gulf of Thailand (GEF ID.5538). We sincerely thank Qin Yu from Sun Yat-sen University for her valuable assistance during this study.

Author contributions

Writing—original draft: Y.Y. and G.L. Investigation: G.L., Z.H., and D.Y. Software: G.L. Data curation: G.L. Formal analysis: G.L. Visualization: G.L. Conceptualization: J.G. and Y.Y. Supervision: J.G. Funding acquisition: J.G. and Y.Y. Resources: J.G. Writing—review and editing: J.G. Methodology: H.Z.

Competing interests

The authors declare no competing interests.

Additional information

Supplementary information The online version contains supplementary material available at https://doi.org/10.1038/s42003-025-08789-z.

Correspondence and requests for materials should be addressed to Guanzhe Li or Jun Gong.

Peer review information *Communications Biology* thanks the anonymous reviewers for their contribution to the peer review of this work. Primary Handling Editors: Linn Hoffmann and Tobias Goris. A peer review file is available.

Reprints and permissions information is available at http://www.nature.com/reprints